

Newsletter

Issue 32, June 2022 Contents

President Report1

Least-squares reverse time migration for flaw characterization using ultrasonic bulk waves11

Data driven based structural damage detection by stochastic Koopman operator and phase space embedding20

Conference News27

Social Media27

Call for Articles28

President Message
Tommy Chan

Professor in Civil Engineering, Queensland University of Technology

Dear All,

First of all, please join with me to congratulate Prof. Hong Hao for winning another award, the Nishino Medal, in the coming The Seventeenth East Asia-Pacific Conference on Structural Engineering and Construction (EASEC-17). Nishino Medal is awarded to a distinguished senior engineer who has been judged to have made internationally recognized contributions in the area of structural engineering and construction through research, development and/or professional practice in the Asia-Pacific region.

Besides, I am also pleased to let you know that the special issue of “Advances in Structural Engineering” in Honor of Professor Hong Hao’s 60th birthday has been published in Volume 25 Issue 7, May 2022 just before his 60th birthday on 29 May 2022. The special issue is to recognize his



Newsletter

enormous contributions to the field of structural dynamics, in particular, blast and impact engineering, earthquake engineering and structural health monitoring (SHM), which is evidenced by his journal publications totaling over 600 by the end of 2021. Prof. Chengqing Wu of University of Technology Sydney stated the following:

He is also a very successful educator and mentor. During the past 25 years, Prof. Hao has nurtured over 50 PhD students to successful completion as the chief supervisor. He has also cultivated 25 post-doctoral fellows. Most of his students are very successful in their respective careers, about half of them are now working in top universities and another half in industry worldwide. They are holding leadership and high academic positions, receiving many research awards with great reputations and recognitions in the profession.

This Special Issue consists of 18 high quality papers contributed by Prof. Hao's collaborators, friends, and former and current students. Details about this special issue can be found in "A Special Issue to Celebrate the 60th Birthday of John Curtin Distinguished Professor Hong Hao (ATSE, FIEAust, FASCE, FISEAM)" in ASE official website:

<https://journals.sagepub.com/toc/ASE/current>"

Prof. Hong Hao, Australian Laureate Fellow, is sitting on our Advisory Board and has been contributing much to ANSHM since its establishment in 2009. I am proud to be his friend and colleague for that many years.

On 17 May, QUT together with the Innovative Manufacturing Cooperative Research Centre (IMCRC) and Monitum, organised an event to launch the Kurloo Technology, which is developed in a three-year \$4.5 million IMCRC collaborative research project collaborating between QUT and a Brisbane-based survey and mapping company Monitum. The QUT research team comprised experts in GNSS, electronics, wireless networks, data science, structural health monitoring and geotechnical engineering, and I am leading the part on the application of the developed technology. The intelligent Internet of Things (IoT) precise positioning sensor devices based on the developed technology have been designed and manufactured by a local manufacturing expertise of [Intellidesign](#).

Newsletter



Photo 1 In the photo I am sitting with my QUT colleague Prof. Yanming Feng (right) with Monitum operations manager Todd Morschel and a Kurloo device.

The Kurloo device is a Global Navigation Satellite System (GNSS) sensor with low-power wireless connection and cloud-based analytics capable of providing near-real-time surface displacement measurements at 3-millimetre precision in three dimensions.

It is a successful example demonstrating how research leads to a commercial product which will be very welcomed by industries ranging from civil construction, transport, and environment to energy, mining, and oil and gas, in which displacement measurements are important for the health and performance monitoring of structures and operations.

Just talking about bridge structures, vertical displacements are one of the most relevant parameters for structural health monitoring of bridges in both the short and long terms. Bridge managers around the globe are always looking for a simple way to measure vertical displacements of bridges. However, it is difficult to carry out such measurements.

The Kurloo device could be an efficient solution to this problem. Collecting information from the



Newsletter

satellite incorporating machine learning techniques could enable its users to have accurate vertical displacement information by just placing the device on a point of interest.

Actually, besides Kurloo Technology, I have also conducted research to obtain accurate vertical displacements using innovative methods. For example, as early as in 2006¹, I had published various papers and introduced two effective methods which could be used to accurately and effectively measure vertical displacement as compared to other traditional methods to obtain such data which are either tedious or expensive². The first method is based on the measured horizontal strains together with the identified curvature functions obtained by a self-developed Fibre Bragg Grating (FBG) Tilt sensors and FBG strain sensors. The second method is using the charge-coupled-device (CCD) camera method that utilizes image processing techniques for pixel identification and subsequent edge detection. These two methods could be considered as pioneering work in vertical displacement measurement. To summarise, the three methods which have been developed to measure vertical displacements are listed as follows:

1. Using GNSS and Machine Learning – Kurloo Technology
2. Using Optical Fibre Sensors
3. Using CCD Camera

All the three methods provide different ways to measure vertical displacements which are all proved to be effective and accurate. It is hard to say which one is the best as it depends on different situations and different application requirements.

The International Association for Structural Control and Monitoring have a conference every 4 years and the next one, 8th World Conference on Structural Control and Monitoring (8WCSCM), will be held in Florida, 5-8 June this year. On 5th of June they will be having a Board meeting and Prof. Bijan Samali was asked to give a 20 min presentation on highlights in Australasian region which is effectively reporting ANSHM activities between 2018 and 2022 (since their last conference). In this

¹ Chan, T.H.T., Tam, H.Y., Chan, T.F. and Lee, P.C. (2006) "Vertical Displacement Measurements for Highway Bridges using Optical Devices/Sensors: A Preliminary Study" Proceedings (CD-ROM) of Asia-Pacific Workshop on Structural Health Monitoring, 4-6 December, Yokohama, Japan, pp. 123-130.

² 142. Chan, Tommy H.T. and Ashebo, Demeke B. and Tam, H.Y. and Yu, Y. and Chan, T.F. and Lee, P.C. and Gracia, Eduardo Perez (2009) "Vertical displacement measurements for bridges using optical fiber sensors and CCD cameras : a preliminary study" Structural Health Monitoring, 8(3). pp. 243-249.

Newsletter

regard, I helped prepare a summary of our activities in the last 4 years. Since it has been prepared, I would like to give the summary described here.

i. Growth of ANSHM in terms of the number of organisations that ANSHM members are affiliated with:

2018	2022	
<ul style="list-style-type: none"> ▪ No. of Universities: 19 ▪ No. of Private Companies: 11 ▪ No. of Road Authorities: 6 ▪ No. of Research Institutes: 3 		<ul style="list-style-type: none"> ▪ No. of Universities: 21 ▪ No. of Private Companies: 27 ▪ No. of Road Authorities: 6 ▪ No. of Research Institutes: 3
Total No. of Organisations: 39		Total No. of Organisations: 57

ii. ANSHM Workshops (2018-2022)

- 2018
 - ANSHM ARC ITTC Workshops



Melbourne (17 Jul 2018)



Brisbane (21 Aug 2018)



Sydney (11 Oct 2018)



Newsletter

- 10th ANSHM Workshop which was held jointly with the 5th Workshop of the Australian Chapter of the International Association of Protective Structures (IAPS-AUS), 10-11 Dec 2018, Wollongong



- 2019
 - 11th ANSHM Workshop to celebrate ANSHM 10th Anniversary, hosted by Griffith University, 2-3 December 2019

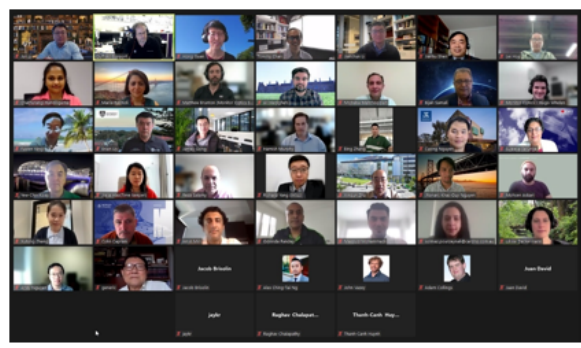


Newsletter

- 2020
 - 12th ANSHM Workshop (online) organised by ANSHM Executive Committee, 7-8 December 2020



- 2021
 - 13th ANSHM Workshop (online) jointly organised by School of Civil and Environmental Engineering, University of Technology Sydney and School of Civil Engineering, University of Sydney on behalf of ANSHM



iii. ANSHM Publications (2018-2022)

- Special Issues
 - A Special Issue on Recent Research Advances on Structural Health Monitoring of Civil Engineering Structures, International Journal of Structural Stability and Dynamics Vol. 20, No. 10 in 2020
 - A Special Issue on Structural identification and evaluation for SHM applications, Journal of Civil Structural Health Monitoring Vol. 8, Issue 5 in 2018
- Quarterly Newsletter
 - 18 Issues Published



Newsletter

- Issue No. 15 (March 2018) to Issue No. 32 (June 2022)
- Edited Book
 - Recent Advances in Structural Health Monitoring Research in Australia, celebrating 10th ANSHM Anniversary, to be published in July 2022
- Research Fundings Secured by ANSHM Members
(A total of an amount of \$15,288,164.00)
- ARC Discovery Projects
 - 11 Projects for a total of ARC funding of A\$5,618,687
- ARC Linkage Projects
 - 2 Projects for a total of ARC funding of A\$663,385
- ARC Industry Transformation Research Hub
 - 1 Project for a total of ARC funding of A\$4,980,000
- ARC Linkage Infrastructure, Equipment and Facilities Projects
 - 2 Projects for a total of ARC funding of A\$1,425,017
- ARC DECRA Projects
 - 2 Projects for a total of ARC funding of A\$780,075
- ARC Future Fellowship Project
 - 1 Project for a total of ARC funding of A\$ 821,000
- IMCRC Project
 - 1 Project for a total of IMCRC funding of A\$ 1,000,000

It seems that although we have been seriously affected by the pandemic, we have also achieved a lot in these four years. All these are due to the efforts of ANSHM Executive Committee members and ANSHM Advisory Board members.

Below are the updates of the month.

ANSHM Workshops

Some updates regarding the 14th ANSHM Workshop as follows:

- The date of 14th ANSHM workshop is likely to be on 24th (Thursday) – 25th (Friday) November, because of some key Advisory Board members are attending another conference organised by Western Sydney University, which is on 28-30 Nov 2022. The Advisory Board members will be consulted to confirm the date.

Newsletter

- Besides, the 14th ANSHM workshop will be held in a hybrid mode (physical + virtual). The venue of the workshop will be likely at Arial Function Centre in UTS.
- It is proposed that the 2-day workshop will be divided into two parts: the first day - a summit on digital transformation of infrastructure assets and the 2nd day - a usual workshop plus AGM and board meeting.

Please email Prof. Li (Jianchun.Li@uts.edu.au) and cc myself (tommy.chan@qut.edu.au) for any suggestion and opinion on this. More details will be provided in the coming months after the venue, dates, etc. have been confirmed.

ANSHM 2nd Monograph

The NOVA art department sent us the book cover design on 25 May 2022 for approval within 72 hours. We got back to them requesting editors' bios to appear on the back cover, and use Brisbane Story Bridge image instead of Sydney Harbour Bridge image, as the latter has been used in our first NOVA book. They sent us the next version on 27 May 2022 addressing our request. The book will come to the final stage of printing after finalising the book cover. The book's expected publication date is late July 2022.

In my last month updates, it was mentioned a special 30% pre-publication discount is available for all orders placed and paid for before the book goes to press as long as ordered by 18 May 2022. I have tried just now (31 May 2022) and it seems that the pre-publication discount is still available. In order to take advantage of this offer, please place your order via the link [Recent Advances in Structural Health Monitoring Research in Australia – Nova Science Publishers \(novapublishers.com\)](https://www.novapublishers.com) and use the code **prepub30** at checkout and I am not sure when this discount becomes expired.

ANSHM Webpage

Thank Prof. Hong Guan and her team so much for faithfully updating the ANSHM Page. It's mentioned above that research grants from members of ANSHM have been successfully updated. One could visit ANSHM Homepage (www.ANSHM.org.au) for details referring to "Current Projects" on the Homepage.

Research Collaboration

Previously, I mentioned about that we look forward to establishing a very strong collaboration platform within ANSHM and with the ARC Industry Transformation Research Hub on Resilient and Intelligent Infrastructure Systems in urban resources and energy sectors (RIIS in short). Prof. Bijan

Newsletter

Samali and myself are the two Leaders of the *Theme 4 Infrastructure Health Monitoring and Predictive Maintenance* of the RIIS Hub. However, the signing of all the agreements with the universities and the industry partner involved although complicated, yet nearly all the agreements have been signed and it is expected that the Hub could be officially started in July 2022. Please visit <https://riis.org.au/> for more details.

ANSHM Who's Who

As mentioned earlier, we will prepare Who's Who of SHM in Australia for people to better understand what we have been doing and what we have achieved, plus a directory of our expertise in various areas of SHM. Prof. Jianchun Li and A/Prof. Jun Li are working on that. They will proceed the task by collecting individual information from ANSHM members who wish to be included, using a designed template, which will be prepared by them. Then the template will be sent to ANSHM EC/AB members for feedback and comments. After that, an email will be sent to all members with the template to collect the required information. The team will use the information to form a single A4 page for each person.

The ANSHM Newsletter

In the next sections, we will have two articles from our members. The first article is written by Dr Jing Rao at the University of New South Wales and the second article is written by the researchers from the Curtin University. Dr. Rao presented a least-squares reverse time migration (LSRTM) algorithm for flaw characterization using ultrasonic bulk waves. Peng et al. presented a data driven based method based on Koopman operator and phase space for developing a damage index which is sensitive to detect structural damage, but insensitive to environmental condition and measurement noise. Please enjoy the reading!

Stay safe and healthy!

With kind regards,

Professor Tommy H.T. Chan PhD, ThM, MDiv, BE (Hons I), FHKIE, MIE Aust, CP Eng, NPER, MICE, C Eng, RPE, MCSCE

President ANSHM (www.ANSHM.org.au)

School of Civil & Environmental Engineering, Queensland University of Technology (QUT)

GPO Box 2434, Brisbane, QLD 4001, AUSTRALIA.

Ph. +61 7 3138 6732; Fax. +61 7 3138 1170; email: tommy.chan@qut.edu.au;

[Research profile](#) | [Research publications](#) | [Google Scholar citations](#)

www.ANSHM.org.au



Newsletter

Least-squares reverse time migration for flaw characterization using ultrasonic bulk waves

Jing Rao

School of Engineering and Information Technology, University of New South Wales, Canberra

E-mail: jing.rao@unsw.edu.au

Abstract – Accurate detection and characterization of complex flaws play an important role in the assessment of structural integrity of critical structures in the aerospace and nuclear industry. In this work, an effective ultrasonic imaging technique based on least-squares reverse time migration (LSRTM) is developed for imaging flaws with irregular shapes. Reverse time migration (RTM) is a powerful wave-equation-based approach and it has the ability to account for rapid spatial velocity variations and to utilize all wavefront information. It is based on cross-correlating the forward wavefield with the back-propagated wavefield scattered from flaws. To achieve images with better quality, the solution can be obtained by iteratively finding an image generating the modeled data which can best match the measured data in a least-squares sense, i.e. least-squares migration (LSM). Combining RTM and LSM, the LSRTM algorithm is applied to the measured data from the virtual experiment and the physical laboratory experiment, and the results show high-quality reconstructed images for irregular flaw identification.

Keywords: Least-squares reverse time migration, ultrasonic imaging, flaw characterization

1. Introduction

Reliable inspection of flaws is very important for the assessment of structural integrity of critical parts in the aerospace, petrochemical and nuclear industry. The type, size and shape of the flaw can assist with the prediction of the remaining life of the parts. A lot of ultrasonic non-destructive evaluation techniques have been shown to be useful for characterizing flaws [1].

There are different ultrasonic sizing techniques, e.g. amplitude, temporal, inversion and imaging, which have been reviewed in detail in [2]. In this work, only imaging methods are considered. Ultrasonic imaging is usually based on ultrasonic arrays, which can be operated by using physical beam forming or full matrix capture (FMC), where the data obtained from all source-receiver pairs is captured [3]. With the FMC data, beam forming or focusing can be used in

Newsletter

post-processing [4]. For example, the popular post-processing methods can be used to size a regularly shaped flaw by measuring the distance between two tips in a focused image if it is embedded [5], or specular reflections from the surface of the flaw if it is surface-breaking [6]. However, characterizing irregularly shaped flaw remains challenging as singly-scattered, refraction and diffraction waves from the flaw have to be considered.

In this work, the least-squares reverse time migration (LSRTM), which was first developed in geophysics [7] is introduced in ultrasonic imaging to size irregularly shaped flaws. The reverse time migration (RTM) technique is based on a two-way wave equation, in which forward extrapolates the wavefield from the source and backward extrapolates the scattered wavefield from the receiver. Extrapolating the time-reversed scattered wavefields by using the finite difference method focuses wave energy toward damaged regions. With the cross-correlation imaging condition [8], the flaw image can be formed via extrapolation. To reduce the artifacts and improve the quality of the image, least-squares migration (LSM) is proposed to match the amplitudes of the modeled data with the measured data via an iterative inversion scheme [9]. Compared with conventional methods that rely on the signal diffracted from the flaw tip, the LSRTM algorithm uses the full wavefield with correct amplitude and phase information, and thus it is capable to characterize irregular-shaped flaws.

This work is organized as follows. The theory of the LSRTM algorithm based on the acoustic approximation is described in Section 2. Finite element modeling and experimental procedures are presented in Section 3. In Section 4, the LSRTM algorithm is applied to the measured data from the virtual experiment as well as the physical laboratory experiment. Conclusions are summarized in Section 5.

2. Least-squares reverse time migration

The process of reverse time migration (RTM) contains three steps: (1) the forward wavefield extrapolation from the source, (2) the extrapolation of time-reversed scattered wavefield from the receiver, and imaging using cross-correlation. Details of the three steps are included in [10]. To improve the image quality, the least-squares migration (LSM) is used to match the amplitudes of the modeled data with the measured data. Combining RTM and LSM, the LSRTM algorithm based on a 2D acoustic equation in frequency-domain with the constant density is presented in this work.

The forward Born modeling can be compactly given by a matrix-vector multiplication [11]

Newsletter

$$\mathbf{d} = \mathbf{L}\mathbf{m}, \quad (1)$$

where \mathbf{L} is the forward Born modeling operator which linearly relates the reflectivity model \mathbf{m} to the measured scattered data \mathbf{d} . Here, each element of the reflectivity model \mathbf{m}_v can be defined as

$$\mathbf{m}_v(\mathbf{x}) = \frac{\delta v(\mathbf{x})}{v_0(\mathbf{x})}. \quad (2)$$

The migrated reflectivity model \mathbf{m}_{mv} can be calculated by using the adjoint \mathbf{L}^T of the forward Born modeling operator to the measured data \mathbf{d} [12]

$$\mathbf{m}_{mv} = \mathbf{L}_v^T \mathbf{d}, \quad (3)$$

where the adjoint \mathbf{L}_v^T is the migration operator related to velocity.

The aim of LSM is to obtain the reflectivity model \mathbf{m}_v by minimizing the difference between the forward modeled data $\mathbf{L}_v \mathbf{m}_v$ and the measured data \mathbf{d} in a least-squares sense

$$f(\mathbf{m}_v) = \frac{1}{2} \|\mathbf{L}_v \mathbf{m}_v - \mathbf{d}\|^2. \quad (4)$$

The minimum of $f(\mathbf{m}_v)$ is achieved when the reflectivity model \mathbf{m}_v satisfies

$$\mathbf{m}_v = (\mathbf{L}_v^T \mathbf{L}_v)^{-1} \mathbf{m}_{mv}, \quad (5)$$

where $\mathbf{L}_v^T \mathbf{L}_v$ is the migration Green's function (or Hessian matrix \mathbf{H}). The Hessian matrix of $\mathbf{L}^T \mathbf{L}$ or \mathbf{H} is usually not an identity matrix, and the main diagonal elements are nonuniform and the off-diagonal elements are nonzero [13].

Directly solving equation (5) needs to explicitly store the Hessian matrix and calculate its inverse, which is memory-consuming and computationally expensive. Equivalently, m_v can be iteratively obtained by solving

$$\mathbf{H}\mathbf{m}_v = \mathbf{m}_{mv}, \quad (6)$$

using a conjugate gradient approach. The implementation flowchart is shown in Table 1. In this work,

Newsletter

implementing the frequency domain LSRTM algorithm with constant density depends on the improved scattering-integral method [11]. The forward Born modeling and the adjoint migration model are based on matrix-vector multiplications, which are carried out by accumulating decomposed vector-scalar products without explicitly constructing or storing matrices.

Table 1: Conjugate gradient approach for solving $\mathbf{H}\delta\mathbf{m}_{v0} = \mathbf{m}_{mv}$.

1. Starting from initial $\delta\mathbf{m}_{v0}$ and setting the residual vector $r_0 = \mathbf{H}\delta\mathbf{m}_{v0} - \mathbf{m}_{mv}$, initial search direction q_0 is set as r_0 , i. e. $q_0 = -r_0$ and $k = 0$.
2. The scalar $\alpha^{(k)}$ is calculated by using the relationship $\alpha^{(k)} = \frac{r^{T(k)}r^{(k)}}{q^{T(k)}\mathbf{H}q^{(k)}}$.
3. The calculation of $\delta\mathbf{m}_v^{(k+1)}$ is expressed as $\delta\mathbf{m}_v^{(k+1)} = \delta\mathbf{m}_v^{(k)} + \alpha^{(k)}q^{(k)}$.
4. Then, the next residual vector $r^{(k+1)}$ is expressed as $r^{(k+1)} = r^{(k)} + \alpha^{(k)}\mathbf{H}q^{(k)}$.
5. The next step is to compute $\beta^{(k+1)}$, which is used to search the next direction $\beta^{(k+1)} = \frac{r^{T(k+1)}r^{(k+1)}}{r^{T(k)}r^{(k)}}$.
6. The next search direction $q^{(k+1)}$ is obtained by using this scalar $\beta^{(k+1)}$, $q^{(k+1)} = -r^{(k+1)} + \beta^{(k+1)}q^{(k)}$.
7. Then, $k = k + 1$, the next scale $\alpha^{(k+1)}$ is computed by using the obtained search direction $q^{(k+1)}$ and this process is repeated.

3. Testing approach

3.1 Finite element simulation

2D finite element simulations implemented in ABAQUS are carried out in an aluminum sample (longitudinal wave velocity=6190 m/s, density=2700 kg/m³ and Poisson’s ratio=0.33) with the size of 200 mm × 50 mm, as shown in Figure 1. Four-node plane strain elements with the size of 0.1 mm are used in the mesh, which ensures more than 30 elements per wavelength of the longitudinal wave at 2 MHz ($\lambda = 3.1$ mm). A flaw with V shape is modeled by removing elements from the mesh. The linear array has 64 elements on the top surface, which are spaced at a fixed pitch of 1.5 mm. The wave generated by the array is a 2-cycle Hann-windowed tone-burst with a centre frequency of 2 MHz. The full matrix capture (FMC) data is collected by using each element as a source to excite ultrasonic waves and all the elements in the array as receivers.

Newsletter

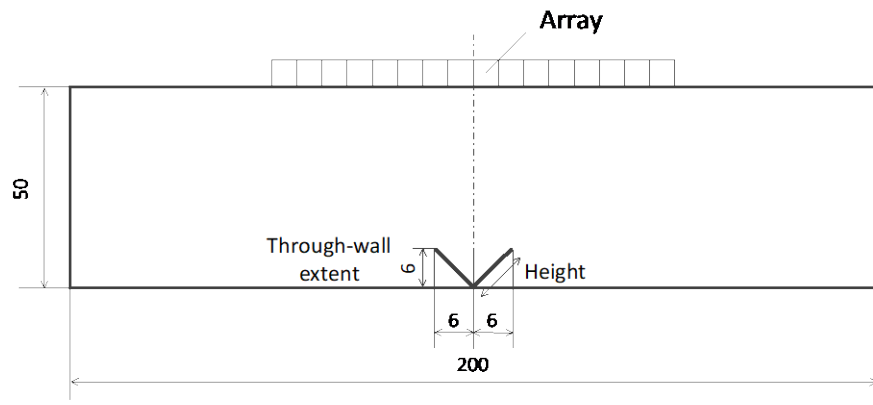


Figure 1: The configuration of an array and a V-shaped flaw. The unit in the figure is mm.

In this case, the signals from the scattering of the flaw will overlap with the reflection from the backwall, and therefore likely to be shadowed. In the virtual experiment, one possible way of extracting scattered fields from the flaw is to obtain the backwall reflection from a flaw-free sample and then subtract it from the overall signal, which is often called the baseline subtraction. However, this way is not practical in a real case, and thus another method will be described in the real physical experiment in Section 3.2. It should be noted that only longitudinal waves are considered in this work, and they can be easily gated from time of arrivals.

3.2 Experimental setup

The experimental setup is shown in Figure 2. The real physical experiment was carried out in a 25 mm thick aluminum block with a width of 200 mm and a height of 50 mm. A V-shaped flaw with a width of 1 mm and a through-wall extent of 6 mm was machined in the block, as shown in Figure 2. The ultrasonic array with a central frequency of 2 MHz manufactured by Guangzhou Doppler Electronic Technologies Co., Ltd was used to excite and receive signals. It has the same number of elements and element pitch as in the virtual experiment. A 5-cycle Hann-windowed tone-burst signal centered at the frequency of 2 MHz was generated from a phased array controller (Lecoeur Electronique, France).



Newsletter

In real inspection, the method of baseline subtraction is not practical because it is not possible to obtain a flaw-free copy of the structure. Therefore, FMC subtraction developed by Zhang *et al.* [14] is used to remove the backwall reflections when flaw signals overlap with backwall reflections. In FMC subtraction, when the element pairs are with the same lateral separation, the length of ray paths of backwall reflections are the same but ray paths of flaw signals are different (see Figure 4(a) in [14]). This means that signals from the backwall have the same arrival time and amplitude compared with the ones from the flaw. Therefore, by subtracting the estimated backwall reflection from the total field, the signal scattered from the flaw can be extracted. Figure 3(a) shows a typical contour plot of the displacement signals measured over all receivers in the aluminum block with the flaw in the physical laboratory experiment. The scattering of longitudinal waves caused by the flaw is separated from the measured signals by removing Rayleigh waves with the gating function and by eliminating backwall reflections with FMC subtraction, as shown in Figure 3(b). The extraction of the flaw signals (see Figure 3(b)) achieved by gating function and FMC subtraction is used in the LSRTM technique to directly image the structure.



Figure 2: Experimental setup.

Newsletter

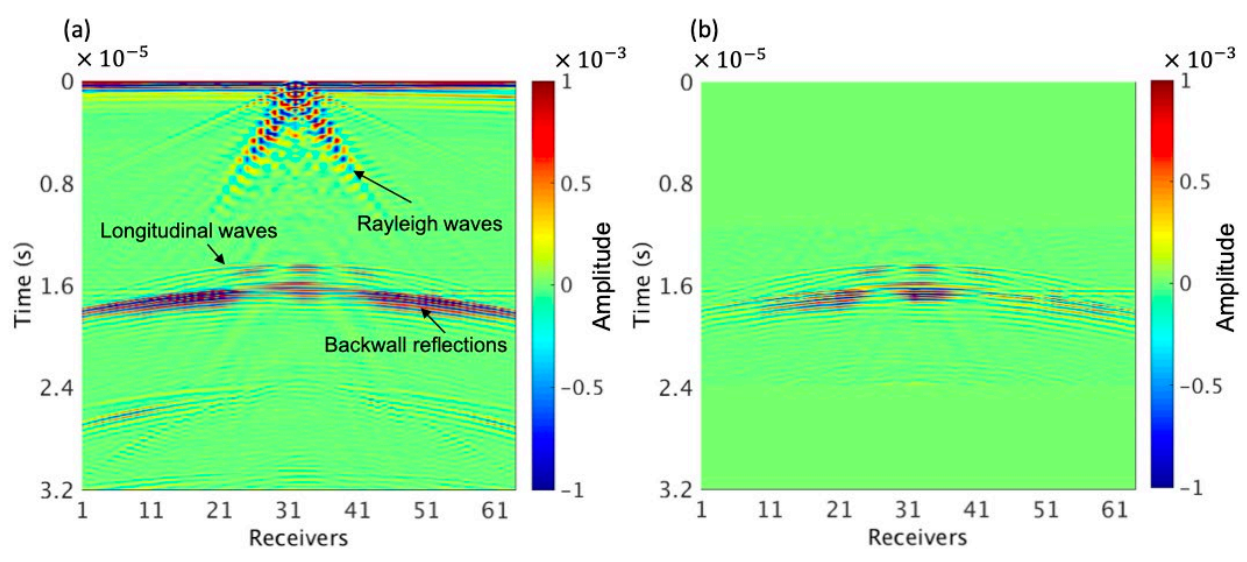


Figure 3: (a) Contour plot of measured displacement excited in one of the array elements. (b) Scattered signals caused by the flaw after time gating and backwall subtraction.

4. Results

The sample with a V-shaped flaw is considered in this work, as shown in Figure 1. Post-processing of the LSRTM images after 10 iterations is done by Laplacian filtering, which is applied to suppress low-wavenumber artifacts. Figures 4(a) and (b) show final images obtained from the virtual experiment and the physical laboratory experiment, respectively. The LSRTM algorithm is performed for 15 frequencies from 0.6 MHz to 3.4 MHz in the virtual experiment, and for 8 frequencies from 1.3 MHz to 2.7 MHz in the physical laboratory experiment, with a frequency interval of 0.2 MHz. The forward model is built by using homogeneous background.

It can be seen from figures that high-quality images are achieved by using the LSRTM algorithm, with the good reconstruction of the shape and the location of the V-shaped flaw in both cases. A clear image is obtained in the virtual experiment, however, the reconstructed width of the flaw is slightly wider than the true model. The reason could be that scattered signals which overlap with mode conversions cannot be accurately separated by using time gating and mode conversions are not considered in the LSRTM algorithm based on the acoustic approximation in this work. In the



Newsletter

physical laboratory experiment, the LSRTM image shows good consistency with the image based on the virtual experiment, although some artifacts are observed and the flaw width is slightly wider. Besides the reason mentioned above, the main reason is the difference between the input waveform used in the LSRTM algorithm and the actual excited waveform in the real physical experiment, which would produce some artifacts to the image. The remaining discrepancy there can be attributed to less frequencies used in the LSRTM imaging from the real physical experiment compared to that from the virtual experiment.

The V-shaped flaw was produced in the controlled laboratory environment and has nominal through-wall extents of 6 mm. The through-wall extent is determined by measuring the vertical distance between the tip and the root of this flaw and is found to be 6.1 mm in the virtual experiment. The through-wall extent is measured to be 6.3 mm from the LSRTM image obtained from the real physical experiment, as shown in Figure 4(b). This result shows a good agreement with the result from the virtual experiment.

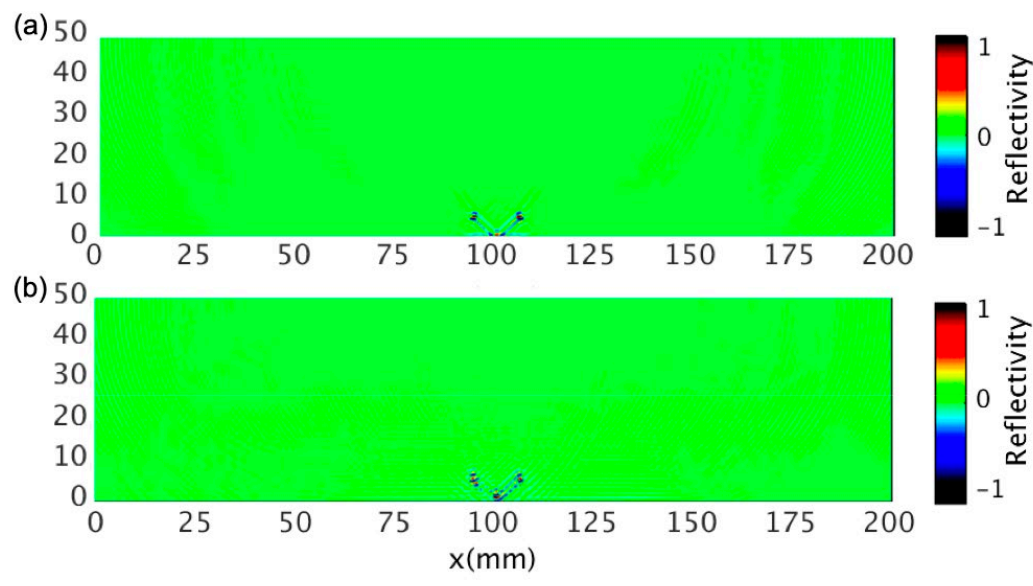


Figure 4: LSRTM images of a V shaped flaw from (a) the virtual experiment and (b) the physical laboratory experiment.

Newsletter

5. Conclusions

In this work, the least-squares reverse time migration (LSRTM) algorithm is investigated for characterizing irregularly shaped flaw. This algorithm is a two-way wave-equation-based approach and attempts to find the best fit reflectivity model by minimizing the mismatching between the measured and modeled data. The LSRTM has been successfully used in the measured data from the virtual experiment as well as the physical laboratory experiment, and the results have shown good accuracy in determining the size, location and shape of the V-shaped flaw.

References

- [1] Bai, L., Velichko, A. and Drinkwater, B.W. Ultrasonic characterization of crack-like defects using scattering matrix similarity metrics. *IEEE Trans. Ultrason. Ferroelectr. Freq. Control* (2015) 62:545–559.
- [2] Felice, M.V. and Fan, Z. Sizing of flaws using ultrasonic bulk wave testing: A review. *Ultrasonics* (2018) 88:26–42.
- [3] Wilcox, P.D. Ultrasonic arrays in NDE: Beyond the B-scan. *AIP Conference Proceedings* (2013) 1511:33–50.
- [4] Holmes, C., Drinkwater, B.W. and Wilcox, P.D. Post-processing of the full matrix of ultrasonic transmit-receive array data for non-destructive evaluation. *NDT & E. Int.* (2005) 38:701–711.
- [5] Holmes, C., Drinkwater, B.W. and Wilcox, P.D. Advanced post-processing for scanned ultrasonic arrays: Application to defect detection and classification in non-destructive evaluation. *Ultrasonics* (2008) 48:636–642.
- [6] Felice, M.V., Velichko, A. and Wilcox, P.D. Accurate depth measurement of small surface-breaking cracks using an ultrasonic array post-processing technique. *NDT & E. Int.* (2014) 68:105–112.
- [7] Dai, W., Fowler, P. and Schuster, G.T. Multi-source least-squares reverse time migration. *Geophys. Prospect* (2012) 60:681–695.
- [8] Claerbout, J.F. Toward a unified theory of reflector mapping. *Geophysics* (1971) 36:467–481.
- [9] Keys, R. and Weglein, A. Generalized linear inversion and the first Born theory for acoustic media. *J. Math. Phys.* (1983) 24:1444–1449.
- [10] Baysal, E., Koslo, D.D. and Sherwoods, J.W.C. Reverse time migration. *Geophysics* (1983) 48:1514–1524.
- [11] Yang, J. Z. and Liu, Y.Z. and Dong, L.G. Least-squares reverse time migration in the presence of density variations. *Geophysics* (2016) 81: S497–S509.
- [12] Claerbout, J.F. *Earth soundings analysis: Processing versus inversion*. Blackwell Scientific Publications, Cambridge, (1992).
- [13] Chavent, G. and Plessix, R.-E. An optimal true-amplitude least squares prestack depth-migration operator. *Geophysics* (1999) 64:508–515.
- [14] Zhang, C., Huthwaite, P. and Lowe, M. The application of the factorization method to the subsurface imaging of surface-breaking cracks. *IEEE Trans. Ultrason. Ferroelectr. Freq. Control* (2018) 65:497–51

Newsletter

Data driven based structural damage detection by stochastic Koopman operator and phase space embedding

Zhen Peng, Jun Li, Hong Hao

*Centre for Infrastructural Monitoring and Protection, School of Civil and Mechanical Engineering,
Curtin University, WA 6102, Australia*

Abstract: Structural health monitoring (SHM) and condition assessment are crucial for ensuring safety and preserving the service life of existing infrastructure. With the superiority in data-driven monitoring strategy which does not require FE modelling and updating, the data feature-based methods have been widely developed in the last decades. This study proposes a novel data driven approach for structural damage assessment based on phase space embedding in conjunction with stochastic Koopman operator. The proposed method is applied to identify damage introduced as the artificially applied settlements of pier in the Z24 benchmark bridge. Results demonstrate that the bridge condition under the reference state and the damage scenarios with different levels of pier settlement are well identified by using the proposed approach with in-field measurement data including different test environment. The defined DSF value can be used to reflect the damage severity in these damage scenarios.

Introduction

Existing infrastructure, such as bridges and buildings exposed to the operational environment for long service life, are prone to performance degradation, owing to material deterioration, natural hazards and human-made loading conditions. Without the need to conduct finite element modelling and the requirement of performing model updating, the data driven damage detection methods provide opportunities to assist real-time and long-term condition assessment of large-scale civil engineering structures. The main objective of data driven-based approaches is to develop damage sensitive features (DSF) that are sensitive to structural condition change, but insensitive to environmental condition and measurement noise. In recent years, phase space trajectory (PST) based damage detection methods have received research attention owing to its much higher sensitivity to structural condition change than traditional modal information based damage features, but a significantly less sensitivity to measurement noise [1]. However, the existing PST-based DSFs are

Newsletter

extracted from the geometry of low dimensional (usually less than or equal to 3) phase space attractor, which is impractical for structures with high dimensional vibration responses under stochastic excitations [2]. Therefore, extending the feasibility and accuracy of PST-based methods to monitor and assess the structural performance under operational conditions is significant and remains largely under-explored. This study proposes a data driven structural damage assessment approach using phase space embedding strategy in conjunction with Koopman operator under stochastic excitations [3].

Signal processing for DSF extraction

The proposed approach consists of three main steps. Firstly, structural vibration responses from a single channel are projected to the dynamic attractor of high dimensional system in phase space using embedding strategy. The second step connects the consecutive embedded Hankel matrix with a mapping matrix, that is, Koopman operator, and obtains the eigenvalues approximation of Koopman operator with subspace DMD. Then, the Mahalanobis distance between the eigenvalue vectors approximated under intact and current testing states is served as DSF to detect the structural condition change.

The phase space attractor of system can be reconstruction from single-channel acceleration measurement $x(t)$ by using Takens' embedding theorems [4]

$$\mathbf{X}_1^m = [\mathbf{x}_1 \ \mathbf{x}_2 \ \dots \ \mathbf{x}_m] = \begin{bmatrix} x(1) & x(1 + \tau) & \dots & x(1 + (m - 1)\tau) \\ x(1 + \tau) & x(1 + 2\tau) & \dots & x(1 + m\tau) \\ \vdots & \vdots & \ddots & \vdots \\ x(1 + (n - 1)\tau) & x(1 + n\tau) & \dots & x(1 + (m + n - 2)\tau) \end{bmatrix} \quad (1)$$

where m and n represent the embedding dimension and the number of samples in each column of the embedding matrix, respectively. Typically, $n \gg m$. τ is the time delay. By introducing an embedding procedure, the single channel vibration response measurement is formed as a higher dimensional attractor in the phase space with more features unfolded [5]. Defining two augmented observation matrices $\mathbf{X}_p^{aug} = [\mathbf{X}_1^m; \mathbf{X}_2^{m+1}]$ and $\mathbf{X}_f^{aug} = [\mathbf{X}_3^{m+2}; \mathbf{X}_4^{m+3}] \in \mathbb{X}^{2n \times m}$, the Koopman operator \mathbf{A}_Ω of measurement subjected to stochastic excitation can be estimated from subspace DMD algorithm.



Newsletter

Furthermore, the eigenvalues, eigenvectors of Koopman operator A_Ω can be calculated from the eigen decomposition. Takeishi et al. [6] compared the subspace DMD with standard DMD, total-least-square DMD and optimized DMD (opt-DMD) to demonstrate the superiority of using subspace DMD in accurately estimating the eigenvalues of several numerical examples corrupted by process noise and observation noise. The pseudo-code of subspace DMD is detailed in Algorithm 1.

Algorithm 1: subspace DMD

Input: augmented Hankel matrix $Y_p^{aug} = [Y_1^m; Y_2^{m+1}]$, $Y_f^{aug} = [Y_3^{m+2}; Y_4^{m+3}]$.

Output: DMD eigenvalues $\tilde{\lambda}_\Omega$, eigenvectors $\tilde{\omega}_\Omega$ and corresponding dynamic mode Φ_Ω .

1: **procedure** subspace DMD (Y_p^{aug}, Y_f^{aug}, r)

2: $[U_{1:r}, S_{1:r}, V_{1:r}] \leftarrow \text{SVD}(Y_p^{aug}, r)$ > $U_{1:r} \in X^{2n \times r}, S_{1:r} \in X^{r \times r}, V_{1:r} \in X^{m \times r}, r = \text{rank}(Y_p^{aug})$

3: $O^{aug} \leftarrow Y_f^{aug} V_{1:r} V_{1:r}^*$ > $O^{aug} \in X^{2n \times r}$

4: $[U_{1:q1}; U_{1:q2}] S_{1:q} V_{1:q}^* \leftarrow \text{SVD}(O^{aug}, q)$ > $U_{1:q1}, U_{1:q2} \in X^{n \times q}, S_{1:q} \in X^{q \times q}, V_{1:q} \in X^{m \times q}$

5: $[\tilde{U}_{1:\tilde{r}}; \tilde{S}_{1:\tilde{r}}; \tilde{V}_{1:\tilde{r}}] \leftarrow \text{SVD}(U_{1:q1}, \tilde{r})$ > $\tilde{U}_{1:\tilde{r}} \in X^{n \times \tilde{r}}, \tilde{S}_{1:\tilde{r}} \in X^{\tilde{r} \times \tilde{r}}, \tilde{V}_{1:\tilde{r}} \in X^{q \times \tilde{r}}, \tilde{r} = \text{rank}(U_{1:q1})$

6: $A_\Omega \stackrel{\text{def}}{=} \tilde{U}_{1:\tilde{r}}^* U_{1:q2} \tilde{V}_{1:\tilde{r}} \tilde{S}_{1:\tilde{r}}^{-1}$ > A_Ω is the stochastic Koopman operator

7: $[\tilde{\omega}_\Omega, \tilde{\lambda}_\Omega] \leftarrow \text{EIG}(A_\Omega)$ > eigenvalues $\tilde{\lambda}$ and eigenvector $\tilde{\omega}$

8: $\Phi_\Omega \leftarrow U_{1:q2} \tilde{V}_{1:\tilde{r}} \tilde{S}_{1:\tilde{r}}^{-1} \tilde{\omega}_\Omega$

9: **end procedure**

The Mahalanobis distance is served as DSF to quantify damage level based on the distance between the eigenvectors obtained from a baseline state and current testing state. From the statistical perspective, the Mahalanobis distance is expressed as

$$d_M(\text{vec}(\tilde{\lambda}_{\Omega(\text{test})})^i) = \sqrt{\text{vec}\{(\tilde{\lambda}_{\Omega(\text{test})})^i - \mu((\tilde{\lambda}_{\Omega(\text{ref})})^i)\}^T [C_{\text{ref}}]^{-1} \text{vec}\{(\tilde{\lambda}_{\Omega(\text{test})})^i - \mu((\tilde{\lambda}_{\Omega(\text{ref})})^i)\}} \quad (2)$$

where $\text{vec}(\cdot)$ is a vectorization operator. The subscripts ‘test’ and ‘ref’ represent the statistical samples

Newsletter

under the testing and reference (healthy) states, respectively, $\mu(\tilde{\lambda}_{\Omega(\text{ref})})$ and C_{ref} denote the mean and covariance of eigenvalues matrix under the reference state, respectively. $(\tilde{\lambda}_{\Omega(\text{test})})^i$ is the i -th eigenvalue vector sample obtained from acceleration responses under the testing state.

In-field Applications of the proposed method

The Z24 bridge is a commonly used benchmark in the civil engineering community for many vibration-based SHM studies including environmental effect analysis, system identification and condition assessment. The front view and top view of the Z24 Bridge are shown in Fig. 1(a). Fig. 1(b) shows the deployment locations of five installed accelerometers during the tests. The vertical acceleration responses at location V2, as shown in Fig. 1(b), under ambient excitations from the reference state and damage scenarios with different levels of settlement of pier, are analysed in this study. Tab. 1 lists the mean values and standard deviations of the first four identified natural frequencies obtained by Stochastic Subspace Identification method, for the reference states and damaged states with pier settlements. Overall, the identified natural frequencies show a slowly decreasing trend with an increasing settlement, under a certain level of uncertainties in the environmental conditions.

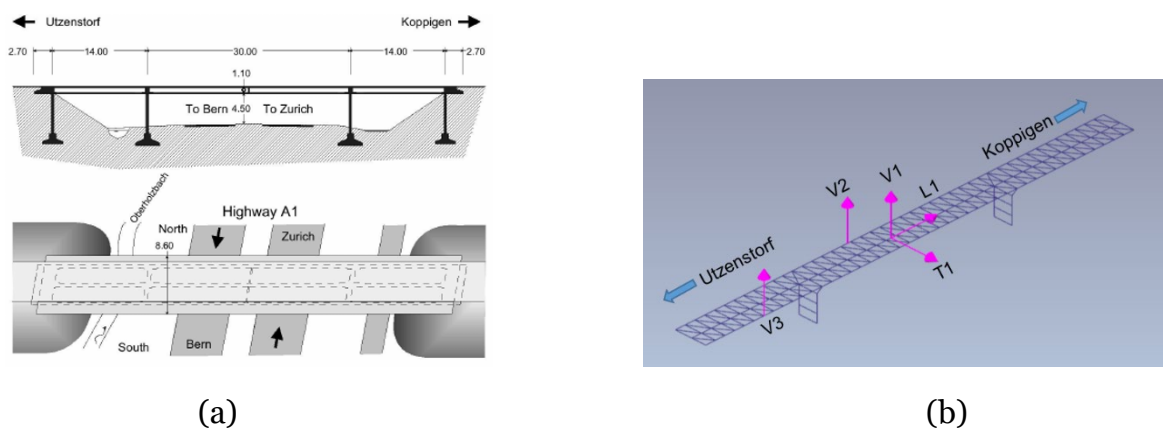


Fig. 1: The Z24 bridge and its sensor locations: (a) Front and top views; (b) Installed accelerometer locations.

Newsletter

Tab. 1: Natural frequencies of Z24 bridge with different pier settlements

No.	Implementation date	Damage scenario	Natural frequency (Hz) (Mean + Std.)			
			Mode 1	Mode 2	Mode 3	Mode 4
1	04/08/1998	First ref. measurement	3.92±0.02	5.12±0.02	9.93±0.02	10.52±0.08
2	09/08/1998	Second ref. measurement	3.89±0.03	5.02±0.04	9.80±0.03	10.30±0.05
3	10/08/1998	Lowering of pier, 20 mm	3.87±0.01	5.06±0.02	9.80±0.04	10.33±0.05
4	12/08/1998	Lowering of pier, 40 mm	3.86±0.01	4.93±0.04	9.74±0.03	10.25±0.03
5	17/08/1998	Lowering of pier, 80 mm	3.76±0.01	5.01±0.03	9.37±0.04	9.90±0.15
6	18/08/1998	Lowering of pier, 95 mm	3.67±0.02	4.95±0.03	9.21±0.04	9.69±0.04

The embedding dimension parameter is set as 40 in this study by using singular value spectrum analysis. In order to formulate the Hankel matrix with the suitable window size, a total of 2000 damage identification trials are conducted for each structural condition with a window size of $n=3000$, $n=4000$ and $n=5000$, respectively. Results are shown in Fig. 2. It is observed that the distribution of DSF values corresponding to the lowering of pier of 40 mm is mixed with that from lowering of pier of 80 mm, when the window size $n \leq 4000$. Good separation results between any two adjacent scenarios are obtained when the window size $n = 5000$. Therefore, a sample window size of 5000 is chosen in this study.

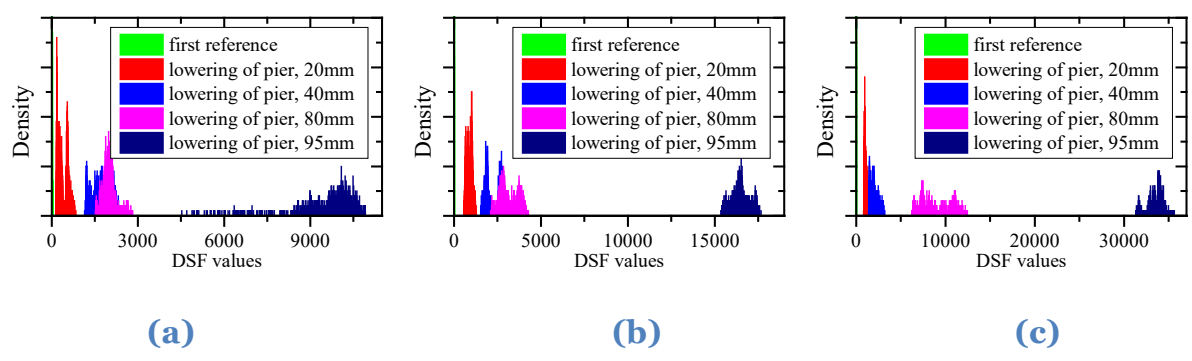
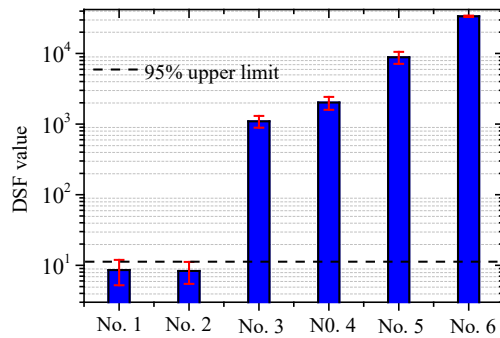


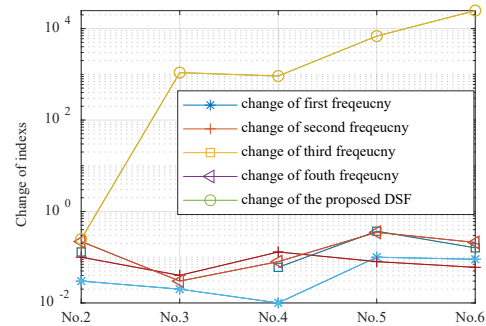
Fig. 2: Distribution of DSF values identified with different window size parameters: (a) $n=3000$; (b) $n=4000$; (c) $n=5000$.



Newsletter



(a)



(b)

Fig. 3: (a) Damage identification results (log-scale) under the reference state and different damage scenarios, (b) Sensitivity analysis and comparison.

Vibration measurement datasets with embedding dimension $m=40$, window size $n=5000$ and unit time lag are analysed for 2000 random trials to statistically obtain the means and standard deviations of DSF values of the bridge under the reference and damaged states. In Fig. 3(a), the DSF values under the reference states from Scenarios 1 and 2 have almost the same values, indicating structural condition is the same. From the results for damage scenarios with settlements of pier, the proposed approach is sensitive to detect the lowering of pier and the corresponding DSF value is obviously increased with the degradation of structural condition. The magnitude of the defined DSF can be used to reflect the severity of the introduced damage. Fig. 3(b) compares the relative change of the proposed DSF and the first four order natural frequencies. It is observed that the proposed DSF is much more sensitive (several order of magnitudes) to detect structural damage than using natural frequencies, even the higher order frequencies.

Conclusion

The main contribution of this study is to obtain the time-invariant stochastic Koopman operator from the phase space representation of observable vibration responses, e.g. a single channel acceleration response, which is subsequently used for damage assessment. The results reveal that the proposed method is sensitive to structural condition change, but insensitive to environmental condition and

Newsletter

measurement noise. In particular, the statistical distribution of the obtained DSF values of each scenario is concentrated and well distinguished, supporting a reliable condition assessment result.

References

- [1] J. Nichols, M. Todd, M. Seaver, L. Virgin, Use of chaotic excitation and attractor property analysis in structural health monitoring, *Physical Review E*, 67 (2003) 016209.
- [2] L. Pamwani, A. Shelke, Damage quantification in moment resisting frame using phase space reconstructed from independent component sources, *Structural Control and Health Monitoring*, 26 (2019) e2438.
- [3] Z. Peng, J. Li, H. Hao, Data driven structural damage assessment using phase space embedding and Koopman operator under stochastic excitations. *Engineering Structures*, 255, (2022) 113906.
- [4] F. Takens, *Detecting strange attractors in turbulence (Lecture Notes in Mathematics)*, Springer, Berlin, 1981.
- [5] D. García, D. Tcherniak, An experimental study on the data-driven structural health monitoring of large wind turbine blades using a single accelerometer and actuator, *Mechanical Systems and Signal Processing*, 127 (2019) 102-119.
- [6] N. Takeishi, Y. Kawahara, T. Yairi, Subspace dynamic mode decomposition for stochastic Koopman analysis, *Physical Review E*, 96 (2017) 033310.

Newsletter

Conference News

- The 8th World Conference on Structural Control and Monitoring, 5-8 June 2022, Orlando, Florida, USA. <http://www.8wcscm.org/>
- Research Symposium on Infrastructure Safety and Resilience, 23 June 2022, Sydney, Australia.
<https://www.eventbrite.com.au/e/research-symposium-on-infrastructure-safety-and-resilience-tickets-349305611487>
- The Seventeenth East Asia-Pacific Conference on Structural Engineering and Construction (EASEC-17) , 27–30 June 2022, Singapore. <https://easec-17.org/index.html>
- The 9th Asia-Pacific Workshop on Structural Health Monitoring, 7-9 December 2022, Cairns, QLD, Australia. <https://www.monash.edu/engineering/shm>

Social Media

Follow us at the next social media and webpages

- ANSHM Facebook webpage: www.facebook.com/ANSHMAU
- ANSHM Facebook group: www.facebook.com/groups/ANSHM
- ANSHM LinkedIn group:
www.linkedin.com/groups/ANSHM-Australian-Network-Structural-Health-4965305

Newsletter

Call for Articles

Interested in publishing an article in ANSHM newsletter, please register here

<https://docs.google.com/document/d/1XJX9qhxEfIkXSVluWDV5rvROuYySM-hWn-q9n8O-Tzw/edit?usp=sharing>

Edition	Submission Deadline	Distribution
Spring	15 Feb	Early March
Summer	15 May	Early June
Fall	15 Aug	Early Sep
Winter	15 Nov	Early Dec

If you have any comments and suggestions, please contact

Newsletter Editors:

Asso/Prof. Jun Li, Curtin University.

Email: junli@curtin.edu.au

Prof. Richard Yang, Western Sydney University.

Email: R.Yang@westernsydney.edu.au

Dr. Mehrisadat Makki Alamdari, University of New South Wales.

Email: m.makkialamdari@unsw.edu.au

Dr. Andy Nguyen, University of Southern Queensland

Email: Andy.Nguyen@usq.edu.au

